J Comp Physiol A (1984) 155:239–247

Journal of Comparative Physiology A Sensory, Neural, and Behavioral Physiology
© Springer-Verlag 1984

Angular sensitivity of blowfly photoreceptors: intracellular measurements and wave-optical predictions

J.G.J. Smakman, J.H. van Hateren, and D.G. Stavenga
Department of Biophysics, Laboratory of General Physics, University of Groningen, Westersingel 34, 9718 CM Groningen, The Netherlands

Accepted June 7, 1984

Summary. 1. The angular sensitivity of blowfly photoreceptors was measured in detail at wavelengths $\lambda = 355$, 494 and 588 nm.
2. The measured curves often showed numerous sidebands, indicating the importance of diffraction by the facet lens.
3. The shape of the angular sensitivity profile is dependent on wavelength. The main peak of the angular sensitivities at the shorter wavelengths was flattened. This phenomenon as well as the overall shape of the main peak can be quantitatively described by a wave-optical theory using realistic values for the optical parameters of the lens-photoreceptor system.
4. At a constant response level of 6 mV (almost dark adapted), the visual acuity of the peripheral cells R1–6 is at longer wavelengths mainly diffraction limited, while at shorter wavelengths the visual acuity is limited by the waveguide properties of the rhabdomere.
5. Closure of the pupil narrows the angular sensitivity profile at the shorter wavelengths. This effect can be fully described by assuming that the intracellular pupil progressively absorbs light from the higher order modes.
6. In light-adapted cells R1–6 the visual acuity is mainly diffraction limited at all wavelengths.

Indroduction

Knowledge of the angular sensitivity of the photoreceptor cells is an essential requirement for understanding spatial information processing by an animal's visual system. The eye of flies is one of the most intensively studied visual systems and the angular sensitivity of single photoreceptors has accordingly been measured by several investigators (e.g. Washizu et al. 1964; Scholes 1969; Streck 1972; Horridge et al. 1976; Hardie 1979). On the other side of the research field, theoretical models of the angular sensitivity of fly photoreceptors have been developed on the basis of the two optical elements involved, the facet lens and the rhabdomere, i.e., the photoreceptor organelle which functions as an optical waveguide (Pask and Snyder 1975; Barrell and Pask 1979; Pask and Barrell 1980a, b).

A critical comparison between theoretical predictions and experimental data has, so far, not been attempted, probably because angular sensitivity measurements with sufficient accuracy were not yet at hand. Recently detailed measurements have become possible through the development of an analog-digital feedback system (Smakman and Pijpker 1983). We report here experimental results obtained from blowfly photoreceptors together with a quantitative theoretical interpretation based on the calculations of van Hateren (1984). Good agreement between theory and experiment could be obtained with realistic assumptions for the optical parameters.

Material and methods

Animals. All experiments were performed on female blowflies *Calliphora erythrocephala* wild type, between 7 and 17 days old. The flies were reared on liver (Razmjoo and Hamdorf 1976), and their high visual pigment content was maintained by keeping the flies under suitable light conditions (see Schwemer 1979, 1983).

Preparation. The flies were prepared for intracellular recordings from the photoreceptor cells along procedures similar to those of Hardie (1979). In brief, a tiny piece of the cornea in the dorsal part of the right eye was removed with a razor blade fragment. The opening was immediately covered with a small drop of vacuum silicone grease. Subsequently the fly was mounted in the centre of a goniometer platform and a glass microelectrode was lowered vertically through the hole in the cornea. The reference electrode

was a sharpened silver wire which was placed in an unstimulated ventral part of the same eye.

The first attempts to measure accurate angular sensitivities in such preparations gave results heavily distorted by the substantial retinal movements typical of fly eyes (see for example Kirschfeld and Franceschini 1969). Several approaches were undertaken to minimize the retinal movements, such as cooling of the fly, anaesthesia and surgery. These procedures, however, all affected the integrity of the dioptric system and were therefore abandoned. The treatment which, finally and fortunately, proved to be successful was a slight pulling out of the antennae (about 0.5 mm) and subsequently securing the antennae base to the extended position with wax. Presumably the eye muscles which are attached to the retinal basal membrane (Hengstenberg 1971) thus are held in a strained state; whatever the mechanism, the angular sensitivity profiles measured from flies with pulled out and fixed antennae were essentially identical to those from flies with fixed antennae that were not pulled out, except for the much improved reproducibility of the curves in the former case. This result was in accordance with checks on the optical qualities of the eye. The slight extension of the antennae did not affect the far-field radiation pattern of the photoreceptors, nor did it change the clarity of the deep-pseudopupil (see Franceschini 1975).

Recording. The experiments were performed in a conventional set-up for intracellular electrophysiology, consisting of a laboratory-made microelectrode amplifier (Muijser 1979) and a storage oscilloscope (Tektronix). The 3 mol/l KAc-filled electrodes had 150–200 MΩ resistance in Ringer's solution and a tip diameter of less than 0.1 μm.

Angular sensitivity measurements. The principle of determining the angular sensitivity of a photoreceptor cell is to scan the visual field of the cell with an infinitely distant point source and to monitor simultaneously its light response. The experimental set-up for measuring the light response is shown in Fig. 1. A monochromatic light beam, obtained by filtering a 450 W Xenon arc (Osram) with a narrow (15 nm) band interference filter (Schott), was focussed on a flexible lightguide which was coupled to a motor-driven perimeter. The aperture of the lightguide was 0.2° as seen by the fly.

After successful penetration of a cell the goniometer platform with fly and intracellular microelectrode was adjusted for maximum response. Then scans of the visual field of the cell were made by moving the lightguide in either the horizontal or the vertical plane. Great care was taken to assure that scanning occurred over the top of the spatial sensitivity distribution, i.e., in a plane containing the visual axis.

Angular sensitivity profiles were measured by a constant criterion method. The light response of the cell was clamped to a constant value by an analog-digital feedback system in which a neutral density wedge controlled the intensity $I(\Phi)$ of the stimulating beam when the angle of incidence varied. The normalized reciprocal of $I(\Phi)$ then yields the angular sensitivity function $S(\Phi) = I(0)/I(\Phi)$. The range of the curves, about three log units, was determined by the range of the wedge.

The analog-digital feedback system. The feedback system consists of the receptor cell, a differential sampler, a digital integrator and a servo-system controlling the neutral density wedge (Fig. 1); for a detailed description see Smakman and Pijpker (1983). A chopped light stimulus (50% light, 50% dark) is delivered to a photoreceptor cell. The membrane potential of the photoreceptor is sampled by the differential sampler, consisting of two separate integrators which integrate the membrane potential over adjustable periods during light and dark respectively. By subtracting the dark voltage from the light voltage the differential sampler thus yields the 'light response' of the receptor cell. This signal then drives the neutral density wedge by means of the digital integrator and the servo-circuit. By constantly comparing the signal to a pre-set reference voltage the light response was clamped.

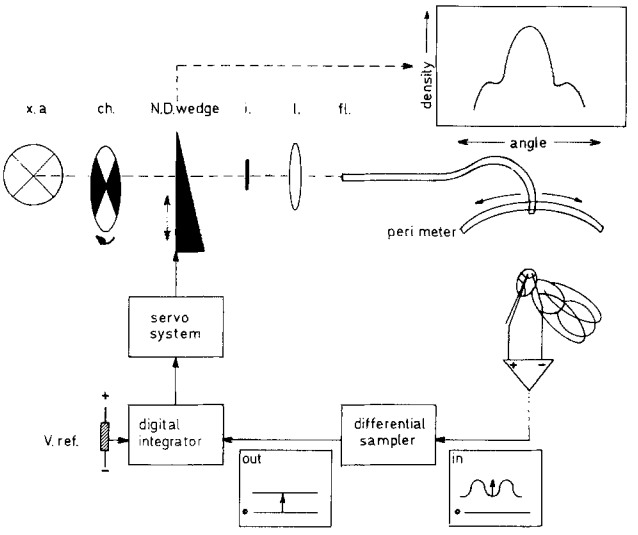

Fig. 1. The analog-digital feedback system used in the angular sensitivity measurements. *x.a*=Xenon arc lamp; *ch*=chopper wheel; *N.D.* wedge=neutral density wedge; *i*=interference filter; *l*=lens focussing the beam at the entrance of flexible light guide *fl.* The response of the photoreceptor to the chopped stimulus is sampled by the differential sampler and via a digital integrator compared with a reference voltage *V* ref. Feedback via a servo system and the neutral density wedge keeps the light response constant. The position of the wedge is a measure for the sensitivity of the photoreceptor cell

Evaluation of the experimental curves. The logarithm of the experimental angular sensitivity was directly registrated on a X-Y recorder (Kipp and Zonen) by recording the position of the neutral density wedge. Actually the shape of the wedge density was not identical for the various wavelengths. This variation is accounted for in the coordinates of the experimental curves in Figs. 3–5, noticeable in the compression of the coordinate values towards the shorter wavelengths. Furthermore, the dependence of the density on wedge position slightly deviated from the ideal linear dependence. The measured angular sensitivities were corrected for both deviations before the theoretical fits were undertaken.

Only data from cells yielding approximately symmetrical angular sensitivity profiles at all applied wavelengths were processed. At every wavelength measured there were made two scans, back and forth through the visual field of the cell. The amplitude of these measured angular sensitivity profiles was evaluated every 0.05°. The mean values were calculated out of the four measured halves of the profile. These mean values were then fit by theoretical curves as described in the next section.

Theoretical analysis. The point light source causes an Airy diffraction pattern in the focal plane of the facet lens. This pattern moves across the rhabdomere tip when the light source scans the visual field of the cell (see Fig. 2). The light distribution at the rhabdomere entrance, together with its waveguide properties, determines the amount of light power which will be propagated in the rhabdomere. Absorption of the propagated light by the visual pigment then is capable of inducing a change in the membrane potential of the cell.

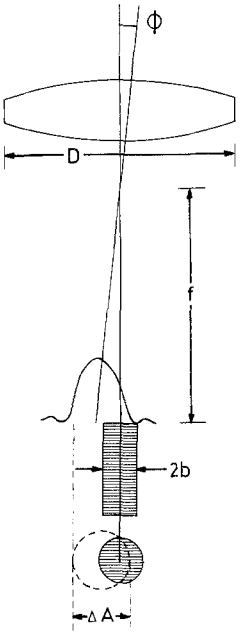

Fig. 2. Optical arrangement of lens and optical waveguide in a fly's eye. D lens diameter; f focal length (in air); b radius of the waveguide; Φ direction angle of incident plane wave. The plane wave is projected as an Airy diffraction pattern in the focal plane, which is coincident with the tip of the waveguide (after Horridge et al. 1976)

The theory (van Hateren, in preparation) for excitation of waveguide modes by an Airy diffraction pattern contains four free parameters: the lens diameter D, the F-number of the lens ($F=f/d$ with f the focal length), the radius of the waveguide b, and $(n_1^2-n_2^2)^{1/2}$, where n_1 and n_2 are the refractive indices of the medium within and surrounding the waveguide respectively. The range within which the parameters can be varied is, however, limited (e.g. Kirschfeld and Snyder 1975).

The value of the V-number, $V=2\pi b\,(n_1^2-n_2^2)^{1/2}/\lambda$ determines the number and shape of allowed modes (see Snyder and Menzel 1975). When $V<2.4$ only the first mode exists (mode 01; Marcuse 1974). When the V-number exceeds the value $V=2.4$ the second mode (mode 11) can be excited and when the V-number exceeds the value $V=3.8$ the third mode (mode 21) can be excited too. From $V=3.8$ a mode 02 can also be excited. This mode was neglected here because, using the parameters discussed below, it is only weakly excited and absorbed in the fly's eye.

The total light power which has passed the facet lens is distributed in an Airy pattern in the focal plane of that lens. The fraction of the power in the Airy pattern that is excited in a mode we call here the excitation efficiency of that mode; so the excitation efficiency of a mode is the fraction of the incident light that can be propagated by that mode along the rhabdomere. However, the contribution of a mode to the angular sensitivity depends on the fraction of the mode that is absorbed by the visual pigment rather than simply propagated. The shape of the angular sensitivity profile depends thus on the relation between the absorbed fractions of the modes concerned. Absorption itself and tapering of the rhabdomere (Boschek 1971) affects the absorption of the different modes in different degrees. It was impossible to calculate these absorbed fractions accurately because the exact parameters that describe the tapering and the absorption are unknown. By adding a suitable amount of the higher order modes to the angular sensitivity function acceptable fits were obtained.

We recall here that when $V<2.4$ only the first order mode exists. This simplest case is encountered at 588 nm, as follows from reasonable estimates of the parameter values (Kirschfeld and Snyder 1975; Beersma et al. 1982). The first step was therefore to create a family of curves for $\lambda=588$ nm. The shape of the calculated angular sensitivity in fact varies little within the plausible ranges of rhabdomere radius b, facet lens F-number and $(n_1^2-n_2^2)^{1/2}$, whereas the shape is sensitive to a change in diameter D. From the family of curves belonging to various D-values we selected (by eye) the curve with the best fit to the experimental data. The corresponding D-value then was used in the next stage of the fit analysis.

We now consider the calculation of the angular sensitivity at $\lambda=355$ nm. In this phase it proved necessary to fix the values of $(n_1^2-n_2^2)^{1/2}$ and the F-number. According to Beersma et al. (1982) for blowfly rhabdomeres $(n_1^2-n_2^2)^{1/2}=0.25$ and, furthermore, preliminary optical measurements on blowfly eyes yielded as a fair estimate $F=2.5$. The rhabdomere radius b could then be easily assessed by comparing again the experimental data with a family of theoretical curves. It became rapidly clear that the experimental curves could never be sensibly approximated when a single mode was assumed. Also, from knowing the value of b (Boschek 1971; Kirschfeld and Snyder 1975) it was evident that at 355 nm the V-number had to exceed the value $V=2.4$ and sometimes also had to exceed the value $V=3.8$. Hence the second and third order modes were included in the analysis. The procedure was to calculate the dependence of the excitation of the modes on the angle of light incidence for a range of b-values. With axial illumination ($\Phi = 0°$) the excitation of the second and third order mode always vanished and, therefore, the sensitivity on-axis must be fully attributed to mode 01. After normalization on the contribution by mode 01 to the angular sensitivity this contribution was subtracted from the (also normalized) experimental data, and the shape of the resulting difference curve was compared with the shape of the excitation function of the second mode. Congruence of the curves depended strongly on the choice of b. As before, the value of b corresponding to the best match was taken. In a few cases this analysis led to such a large value for b that, as a consequence, at $\lambda=355$ nm, $V>3.8$; then the third mode, mode 21, becomes allowed. The match between the theoretical curve and the measured angular sensitivity was then improved by adding to the theoretical curve a contribution by the 21-mode.

As noted above, the excitation of the modes only depends on the optical elements involved (i.e. the facet lens and the rhabdomere). The excitation efficiency M_{01}, M_{11} and M_{21} are the maximal excitation efficiencies of the modes 01, 11 and 21 respectively. Figures 3–5 show that the efficiency of excitation for the different modes reaches a maximum at different positions of the stimulus light. This position is on-axis for the first mode and off-axis for the second and third mode. These values are tabulated for each fit. The weighting factors W_{11} and W_{21} of the amplitudes of the second and third mode respectively with respect to the normalized first mode are also tabulated for each fit. The maximal contribution of mode ij to the angular sensitivity profiles equals $(M_{ij}/M_{01})W_{ij}$.

The angular sensitivity measured at $\lambda=494$ nm was fitted subsequently with the acquired values for facet lens D and rhabdomere radius b, together with the chosen values $(n_1^2-n_2^2)^{1/2}=0.25$ and $F=2.5$; the excitation efficiency of mode 01 was calculated and after normalization compared with the experimental curve. In case mode 11 was allowed at 494 nm ($V(\lambda=494\text{ nm})>2.4$) the excitation efficiency of this mode was calculated as well.

We remark here that identical excitation efficiencies result by appropriate scaling. When the F-number is multiplied by a factor q, identical theoretical fits are obtained when simultaneously the rhabdomere radius b is multiplied by q (the relative extension of the Airy pattern and rhabdomere cross-section then remains constant) and $(n_1^2-n_2^2)^{1/2}$ is devided by q (the V-number remains unchanged).

Results

The angular sensitivities presented in Figs. 3–5 were measured on photoreceptor cells in the frontal part of the right eye of female blowflies. Only peripheral photoreceptor cells R1–6 were investigated in detail; the cells were classified from their spectral sensitivity. The level to which the light response was clamped was in all cases 6 mV. Sensitivity profiles obtained with lower clamp levels were less accurate as the noise of the membrane potential deteriorated the recordings; results with 2 or 6 mV criteria respectively were not significantly different except for this difference in noise. Clamp levels above 6 mV did not significantly improve the accuracy.

Recordings from three cells stimulated with light of wavelengths 588, 494 and 355 nm respectively are shown in the upper rows of Figs. 3–5. A main peak together with distinct but much smaller side bands are characteristic features of recordings judged to be from single cells. A complete set of recordings consisted of three scans, back and forth, through the visual field in the horizontal plane at the three wavelengths mentioned, plus a scan in the vertical plane at $\lambda = 494$ nm. The latter scan was performed to check that the visual field of the cell was rotationally symmetrical, and to locate the visual axis so that the plane of the horizontal scans should include this axis.

The shape of the angular sensitivity curves is very reminiscent of the Airy diffraction pattern, especially that for $\lambda = 588$ nm. At this longest wavelength the sidebands are broader and further removed from the visual axis than those measured at shorter wavelengths. In Table 1 the relation between $\Delta\rho$ (the half-width of the curve) and ΔA (the angular distance between first minima) is summarized for the series of angular sensitivity profiles at different wavelengths of eight cells. Only those records which showed clearly symmetrical sidebands were processed. It seems, especially at $\lambda = 588$ nm, quite natural to assume that the angular sensitivity profile is mainly determined by the diffraction pattern, but it is ca. 15% broader (see also van Hateren 1984). Closer scrutiny of the shorter wavelength curves (Figs. 3–5), however, reveals the often flattened shape of the main peak (Table 1). This phenomenon is readily understood when the waveguide properties of the rhabdomere are taken into account, as will be shown below.

Angular sensitivity curves calculated on the basis of a theoretical model (van Hateren, in preparation) comprising both the diffraction at the facet lens and the waveguide optics of the rhabdomere

Table 1. $\Delta A/\Delta\rho$ and the relative height of the first sideband of angular sensitivity profiles of R1–6 cells of *Calliphora*. Presented are the mean values with standard deviation of eight cells at three wavelengths. $\Delta\rho$ is the half-width of the curve; ΔA is the angular distance between the first minima. For a diffraction pattern $\Delta\rho$ equals λ/D and ΔA equals 2.4 λ/D: then $\Delta A/\Delta\rho = 2.4$. The relative height of the first sideband of a diffraction pattern is 1.7%

λ (nm)	$\Delta A/\Delta\rho$	relative height of the first sideband (%)
355	1.9 ± 0.2	3.4 ± 1.4
494	2.3 ± 0.2	2.3 ± 1.1
588	2.5 ± 0.3	2.3 ± 1.7

were fit to the experimental data with the procedure described in the methods section. A very satisfactory correspondence could be achieved for the main peak of all curves (Figs. 3–5). It was not possible to fit the side bands in the angular sensitivity profile with sufficient accuracy. The main reason was that the height of the side bands of the measured angular sensitivity profiles in general were somewhat higher than theoretically predicted (see Table 1). Several factors can be the cause of this failure; for instance very slight inadequacies in the penetration will lead to artificial electrical coupling between cells, genuine cell-cell couplings as well as optical couplings between rhabdomeres may exist, and the assumptions of the theoretical model that the facet lens is circular and aberration free and that the tip of the rhabdomere is situated precisely in the focal plane may not be fulfilled. We conclude, nevertheless, that although the theoretical curves do not approximate the measured angular sensitivity curves over the complete three log unit range, the striking fits in the main peak support the applicability of the theoretical model.

Table 2 summarizes the parameter values derived from the fit procedure for five cells, A–E. The table includes the half-width $\Delta\rho$ of the angular sensitivity curves measured at three wavelengths $\lambda = 588$, 494 and 355 nm (a measurement at $\lambda = 413$ nm was performed for cell D as well), the calculated values of D and b (the bars indicate that values were determined from the fits at 588 nm and 355 nm respectively, and were subsequently fixed), the resulting V-number, the weighting factors W_{11} and W_{12} of the second and third mode, and the maximal excitation efficiencies M_{01}, M_{11} and M_{12} of the first three modes. We recall here that the excitation efficiencies refer to light propagated in the rhabdomere, whereas the weighting factors refer to the fraction of ligth absorbed in the rhabdomere from a higher order mode relative to the fraction absorbed from the first mode.

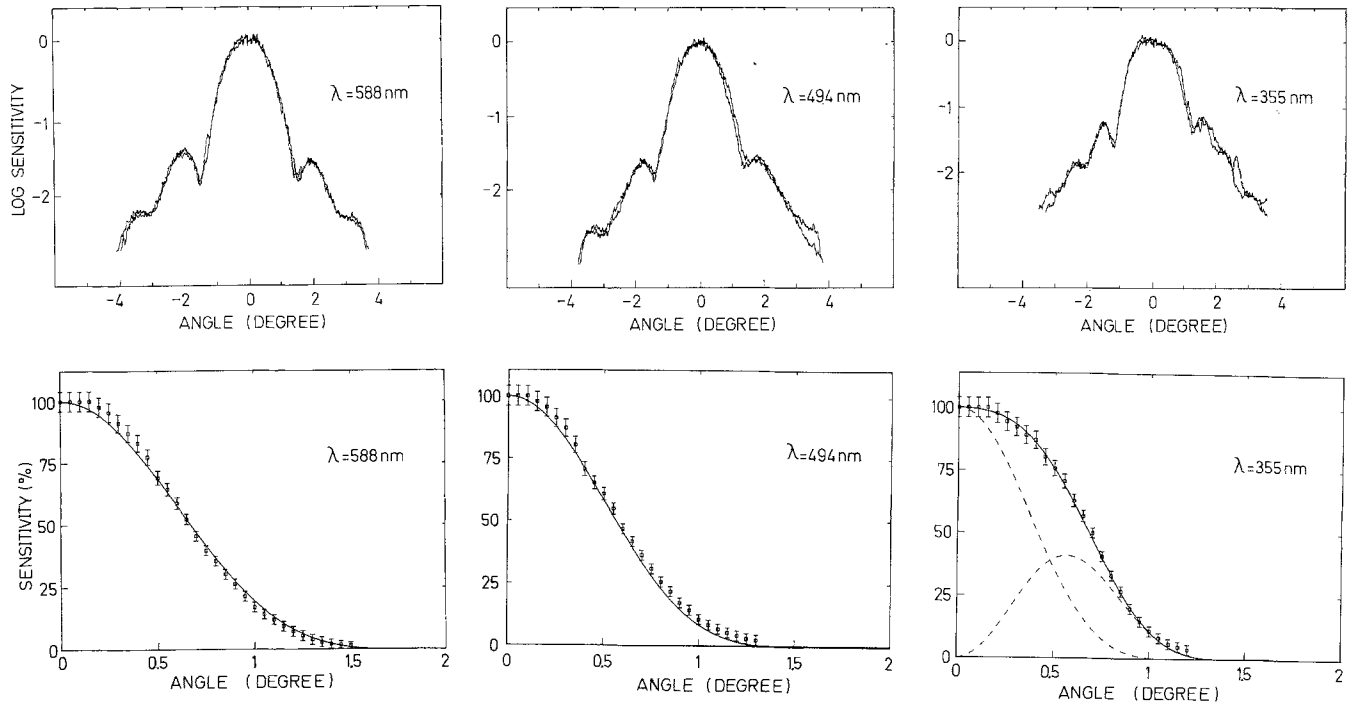

Fig. 3. Angular sensitivities measured at wavelength 588, 494 and 355 nm (upper row) are evaluated (data points with accuracy error) and compared with theoretical fits (lower row). Cell A of Table 2. Note that in the upper row the difference in the coordinate is due to the different shapes of the neutral density wedge at the various wavelengths. Note that the scaling of the coordinate of the upper row is logarithmic and of the lower row is linear. Broken lines indicate contributions of the different modes

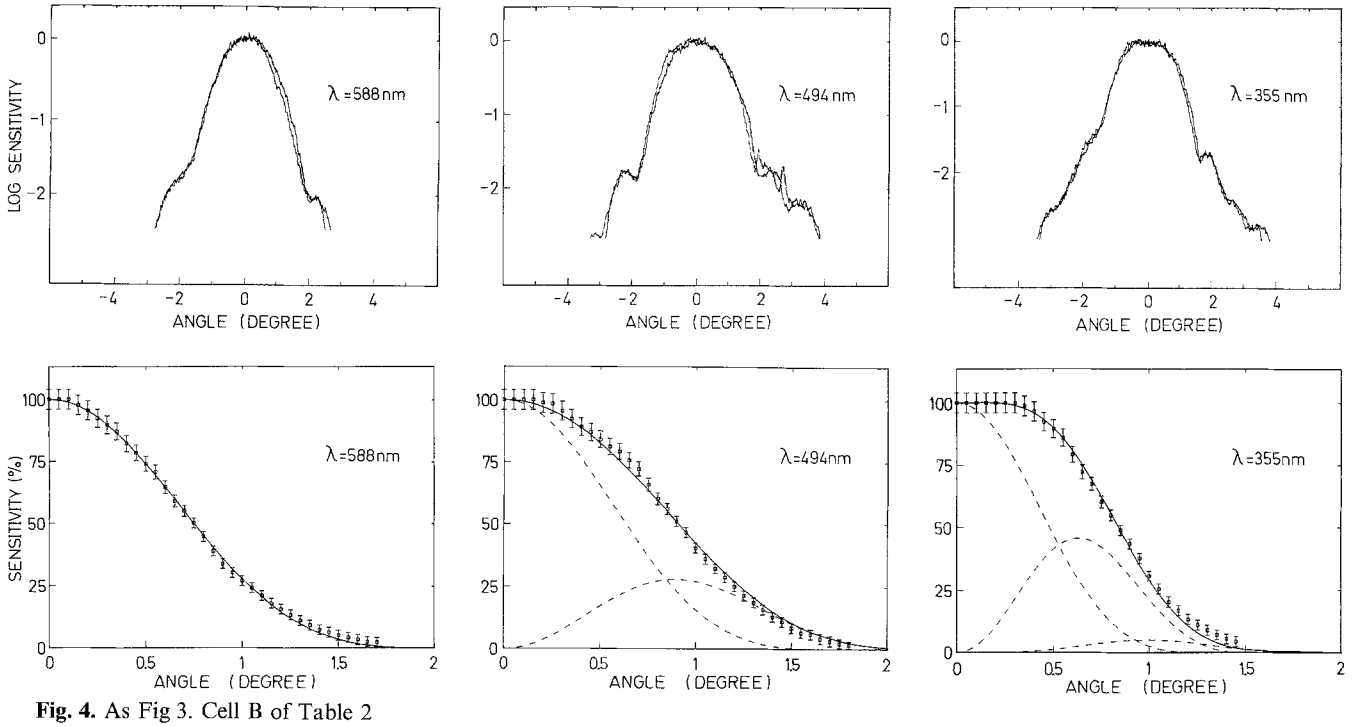

Fig. 4. As Fig 3. Cell B of Table 2

Table 2 shows that the weighting factor W_{11} increases with V. This is directly related to the property of waveguides that the fraction of light power of higher order modes which is propagated inside the waveguide (given by the parameter η, see Snyder and Menzel 1975) increases more strongly with V than does the fraction of light power of the first order mode.

We can conclude from Table 2 that a broad angular sensitivity at 588 nm can be attributed to

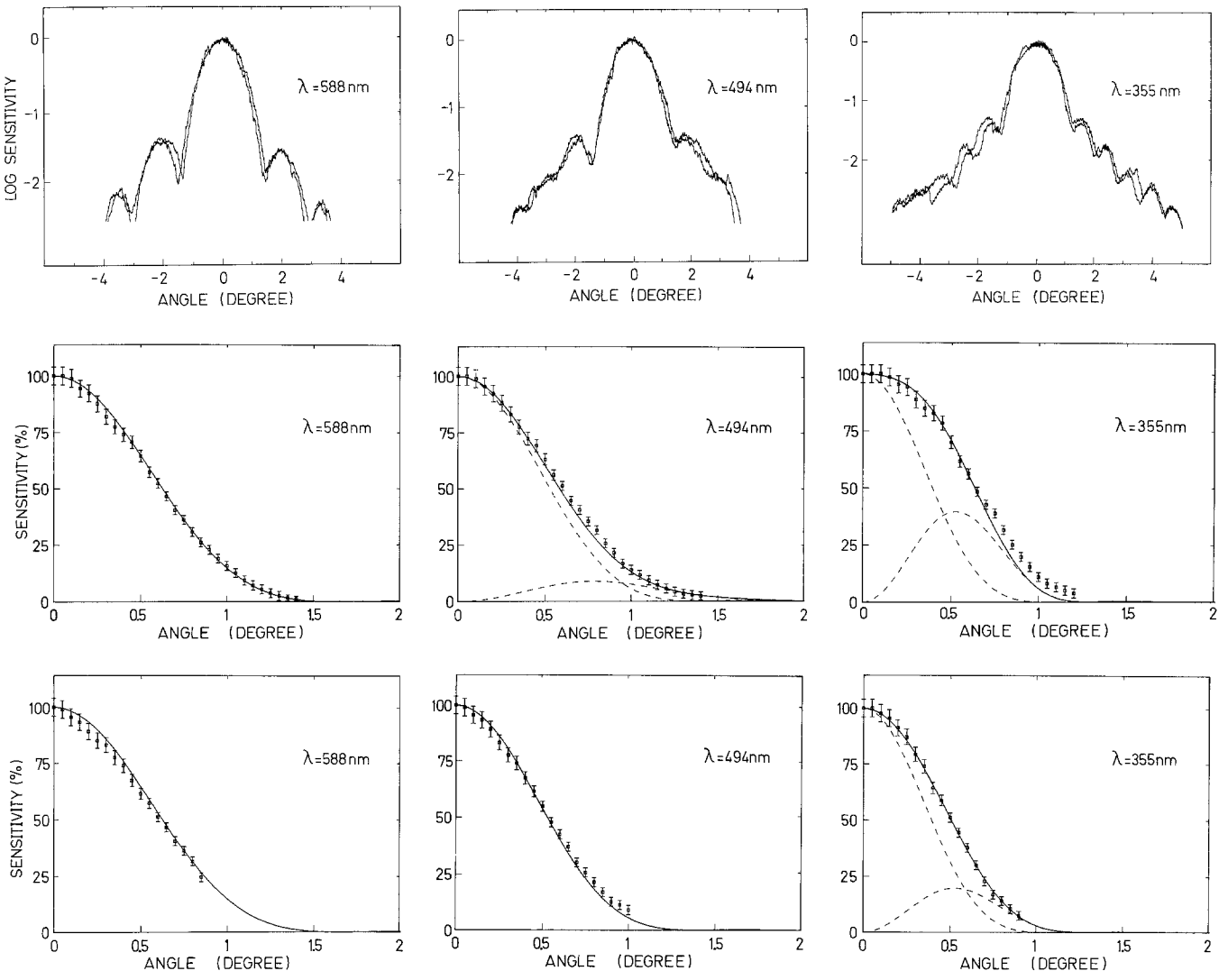

Fig. 5. Cell C of Table 2. Upper row and middle row as the upper row and lower row of Fig. 3. In the lower row are the theoretical fits to data obtained from curves measured in the light adapted state of the same cell C (in Table 2 noted as cell C_p). The narrowing of the angular sensitivities occurring upon light adaptation is presumably caused by the pupil mechanism which reduces the second mode more strongly than the first mode

a small effective diameter of the facet lens (cell D and E), while a narrow angular sensitivity can be attributed to a large effective facet diameter (cell A, B and C). We remark here that cells A, B and C were penetrated frontally, in the area where the facets are large, whereas the location of cells D and E was rather ventral, where the facets are smaller (Kuiper 1966).

We finally remark here that the variation in the angular sensitivity profiles measured at 355 nm corresponds predominantly with a variation in the *V*-value of the rhabdomere, which can be attributed to a variation in the rhabdomere diameters of blowfly R1–6 photoreceptors (see Boschek 1971; Horridge et al. 1976).

Pupil. The cells R1–7 contain pigment granules which migrate upon light adaptation (Kirschfeld and Franceschini 1969) towards the rhabdomere in the distal part of the cell. The pupil acts as a 'longitudinal pupil', i.e., part of the light that is propagated outside the rhabdomere is absorbed. The effective absorbance spectrum of the pupillary granules was determined by Vogt et al. (1982). After pupil activation the spatial sensitivity profile is narrowed (see Beersma 1979; Hardie 1979). We have attempted to interpret this narrowing of the angular sensitivity profile in terms of waveguide optics, using measurements of the angular sensitivity profiles of light adapted cells at different wavelengths. The cells were light adapted with a second light beam

Table 2. A survey of the parameters of the fitted angular sensitivities of five R1–6 cells of *Calliphora*. Cell C_p is cell C light adapted. λ is the wavelength of the stimulus, D the estimated effective diameter of the facet lens, and b the estimated radius of the rhabdomere. The V-number, weighting factors W_{11}, W_{21} and maximal excitation efficiencies M_{01}, M_{11}, M_{21} as well as the measured half-widths of the angular sensitivities are presented here for the wavelengths investigated. For further explanation see text

Cell	λ (nm)	$\Delta\rho$ (°)	D (μm)	b (μm)	V	W_{11}	W_{21}	M_{01}	M_{11}	M_{21}
A	588	1.32	29		2.00	–	–	0.75	–	–
	494	1.15			2.38	–	–	0.78	–	–
	355	1.38		0.75	3.31	0.85	–	0.80	0.39	–
B	588	1.50	26		2.40	–	–	0.78	–	–
	494	1.81			2.86	0.60	–	0.80	0.37	–
	355	1.68		0.90	3.98	0.85	0.20	0.77	0.42	0.20
C	588	1.25	31		2.14	–	–	0.76	–	–
	494	1.22			2.54	0.20	–	0.78	0.34	–
	355	1.27		0.80	3.54	0.80	–	0.80	0.39	–
C_p	588	1.25			2.14	–	–	0.76	–	–
	494	1.07			2.54	–	–	0.78	0.34	–
	355	1.04			3.54	0.40	–	0.80	0.39	–
D	588	1.68	23		2.40	–	–	0.78	–	–
	494	1.94			2.86	0.55	–	0.80	0.37	–
	413	1.83			3.42	0.65	–	0.80	0.39	–
	355	1.86		0.90	3.98	0.85	0.20	0.77	0.42	0.20
E	588	1.81	21		2.00	–	–	0.75	–	–
	494	1.68			2.38	–	–	0.78	–	–
	355	1.94		0.75	3.31	0.80	–	0.80	0.39	–

Table 3. The wavelength dependent narrowing of the angular sensitivity after light adaptation. The relation between the half-width values of the angular sensitivities before and after light adaptation depends on the wavelength of the stimulus. Mean values with standard deviation are presented here ($n=5$)

λ (nm)	$\Delta\rho$ (light)/$\Delta\rho$ (dark)
355	0.73 ± 0.06
494	0.84 ± 0.15
588	0.97 ± 0.07

(550 nm) which generated wide field illumination of sufficient intensity to activate the pupil. The angular sensitivity in the light adapted state can be measured as before, because the differential sampler substracts the voltage induced by the constant beam.

In Table 3 the narrowing of the angular sensitivities is summarized for the three wavelengths, measured for five cells. At 588 nm the angular sensitivity profile is not significantly narrowed after light adaptation, whereas at 494 nm and especially at 355 nm a clear narrowing of the angular sensitivity profile upon light adaptation is observed.

Of the five cells A–E for which a complete set of angular sensitivity profiles for the (approximately) dark adapted state were processed only cell C was also investigated in the light adapted state. The results are presented in the lower row of graphs of Fig. 5. A comparison with the dark adapted cell C (Fig. 5, upper and middle row) reveals that upon light adaptation the angular sensitivity curves of the shorter wavelengths are narrowed (see also the value of the half-width of the angular sensitivity in Table 2). The theoretical fits to both dark and light adapted states of Fig. 5 were performed with identical values for the parameters D, F, b and $(n_1^2-n_2^2)^{1/2}$; thus the excitations of the modes in the dark and light adapted states are identical. The narrowing of the light adapted curves is therefore likely caused by a reduced absorption of light propagating in the second mode relative to the first mode, as represented by the value of W_{11} in Table 2.

Discussion

The analog-digital feedback system for measuring photoreceptor qualities with a constant criterion method developed by Smakman and Pijpker (1983) has provided the facilities to measure angular sensitivities of blowfly photoreceptors with great precision. The data confirm previous assessments of half-width values (e.g. Hardie 1979) being in the range of 1–2°. The essential progress, of course, is that the

present measurements allow a critical appraisal of optical theories for the integrated lens-photoreceptor system (Pask and Snyder 1975; Barrell and Pask 1979; Pask and Barrell 1980a, b; van Hateren 1984).

Horridge et al. (1976) neglected the waveguide properties of the rhabdomere in their analysis of angular sensitivities. If we do this, then to explain our experimental data we would have to assume different diameters of the same rhabdomere at the different wavelengths.

We have shown above that good fits to the experimental data can be derived from the idealizedconception of a perfect lens with in its focal plane the tip of a perfect waveguide. Obviously the electrophysiological experiments strongly support the validity of this theory. The very same model proved to be also adequate for a quantitative description of optically measured angular sensitivities (van Hateren 1984). Obviously, the electrophysiological and optical experiments taken together strongly support the validity of the applied theory. It should be emphasized, however, that the theory is far from exhaustive. For instance, the cross-section of fly rhabdomeres often is slightly elliptical (Boschek 1971; Smola and Wunderer 1981). Furthermore, the media within and surrounding the rhabdomeres are not isotropic and the illumination at the rhabdomere entrance may not be the ideal Airy distribution due to imperfections of the lens. We expect, however, that a theory based on the real physical properties of facet lens and rhabdomere will yield angular sensitivities very similar to those presented here. Again we emphasize that no theory which ignores the waveguide properties of the rhabdomere can succeed.

The angular sensitivity of a fly photoreceptor narrows upon light adaptation (Fig. 5; see Hardie 1979). An obvious candidate explanation of this effect is the pupil mechanism, the assembly of pigment granules inside the photoreceptor cell body which migrate towards the rhabdomere upon light adaptation. The present results cast light on the optical details of the control process since the only difference between the theoretical fits to the dark- and light-adapted states was a smaller contribution from the second mode in the light-adapted state.

A main difference between the first and higher order modes is the larger fraction of lightpower of the latter propagated outside the rhabdomere (Snyder and Menzel 1975). Thus the pigment granules should be relatively more effective in attenuating these higher order modes, as indicated by the angular sensitivity profiles. In fact this explanation was advanced by Snyder and Horridge (1972) for the narrowing of the angular sensitivity curve upon light adaptation of cockroach photoreceptors. In general, light control in photoreceptors may occur also through a variation of refractive indices, but at least in the case of the fly it seems that the effect of the pupillary granules may be understood simply in terms of their absorbing function (for a discussion see also Stavenga 1975, 1979).

After pupil activation the first mode dominates at all wavelengths. In other words, in the light-adapted state the visual acuity is limited mainly by the diffraction pattern at all wavelengths regardless of the rhabdomere diameter. Pupil activation provides an enhancement of the resolving power of the R1–6 cells at the shorter wavelengths.

According to Hardie (1979) the half-widths of the angular sensitivities of the light adapted R1–6 cells are of the same size as those of (dark adapted) R7 and R8 cells. This agreement can be explained, because the smaller diameter of the R7 and R8 rhabdomeres probably only permits excitation of the first mode.

General conclusion

The angular sensitivity profiles of R1–6 cells of the blowfly reported here can be well understood from the physics of a lens-waveguide system. The variability in the shape of the angular sensitivity curves is explained from the variability of the facet lens diameter over the eye and the variability of the rhabdomere diameter among the photoreceptor cells.

Acknowledgements. We thank Dr. W.S. Bialek for valuable comments on the manuscript, Prof. Dr. J.W. Kuiper for continuous stimulating support of this study and Mrs. E. Nienhuis, U.J. Douma and B. Vorenkamp for expert technical assistance. The Dutch Organization for the Advancement of Pure Research (Z.W.O.) provided financial funds.

References

Barrell KF, Pask C (1979) Optical fibre excitation by lenses. Opt Acta 26: 91–108

Beersma DGM (1979) Spatial characteristics of the visual field of flies. Thesis Groningen

Beersma DGM, Hoenders BJ, Huiser AMJ, Toorn P van (1982) Refractive index of the fly rhabdomere. J Opt Soc Am 72: 583–588

Boschek CB (1971) On the fine structure of the peripheral retina and lamina ganglionaris of the fly, *Musca domestica*. Z Zellforsch 118: 369–409

Franceschini N (1975) Sampling of the visual environment by the compound eye of the fly: fundamentals and applications. In: Snyder AW, Menzel R (eds) Photoreceptor optics. Springer, Berlin Heidelberg New York, pp 98–125

Hardie RC (1979) Electrophysiological analysis of fly retina. I:

Comparative properties of R1–6 and R7 and 8. J Comp Physiol 129: 19–33
Hateren JH van (1984) Waveguide theory applied to optically measured angular sensitivities of fly photoreceptors. J Comp Physiol A 154: 761–771
Hengstenberg R (1971) Das Augenmuskelsystem der Stubenfliege *Musca domestica*. I: Analyse der 'clock spikes' und ihrer Quellen. Kybernetik 9: 56–77
Horridge GA, Mimura K, Hardie RC (1976) Fly photoreceptors. III: Angular sensitivity as a function of wavelength and the limits of resolution. Proc R Soc Lond B 194:151–177
Kirschfeld K, Franceschini N (1969) Ein Mechanismus zur Steuerung des Lichtflusses in den Rhabdomeren des Komplexauges von *Musca*. Kybernetik 6: 13–22
Kirschfeld K, Snyder AW (1975) Waveguide mode effects, birefringence and dichroism in fly photoreceptors. In: Snyder AW, Menzel R (eds) Photoreceptor optics. Springer, Berlin Heidelberg New York, pp 56–77
Kuiper JW (1966) On the image formation in a single ommatidium of the compound eye in Diptera. In: Bernhard CG (ed) The functional organization of the compound eye. Pergamon Press, Oxford New York, pp 35–50
Marcuse D (1974) Theory of dielectric optical waveguides. Academic Press, New York
Muijser H (1979) A micro-electrode amplifier with an infinite resistance current source for intracellular measurements of membrane potential and resistance changes under current clamp. Experientia 35: 912–913
Pask C, Barrell KF (1980a) Photoreceptor optics I: Introduction to formalism and excitation in a lens-photoreceptor system. Biol Cybern 36: 1–8
Pask C, Barrell KF (1980b) Photoreceptor optics II: Application to angular sensitivity and other properties of a lens-photoreceptor system. Biol Cybern 36: 9–18
Pask C, Snyder AW (1975) Angular sensitivity of lens-photoreceptor systems. In: Snyder AW, Menzel R (eds) Photoreceptor optics. Springer, Berlin Heidelberg New York, pp 159–166
Razmjoo S, Hamdorf K (1976) Visual sensitivity and the variation of total pigment content in the blowfly photoreceptor membrane. J Comp Physiol 105: 279–286
Scholes J (1969) The electrical responses of the retinal receptors and the lamina in the visual system of the fly *Musca*. Kybernetik 6: 149–162
Schwemer J (1979) Molekulare Grundlagen der Photorezeption bei der Schmeissfliege *Calliphora erythrocephala* Meig. Habilitationsschrift, Ruhr Universität, Bochum
Schwemer J (1983) Pathways of visual pigment regeneration in fly photoreceptor cells. Biophys Struct Mech 9: 287–298
Smakman JGJ, Pijpker BA (1983) An analog-digital feedback system for measuring photoreceptor properties with an equal response method. J Neurosci Meth 8: 365–373
Smola U, Wunderer H (1981) Fly rhabdomeres twist in vivo. J Comp Physiol 142: 43–49
Snyder AW, Horridge GA (1972) The optical function of changes in the medium surrounding the cockroach rhabdom. J Comp Physiol 81: 1–8
Snyder AW, Menzel R (eds) (1975) Photoreceptor optics. Springer, Berlin Heidelberg New York
Stavenga DG (1975) Optical qualities of the fly eye. An approach from the side of geometrical, physical and waveguide optics. In: Snyder AW, Menzel R (eds) Photoreceptor optics. Springer, Berlin Heidelberg New York, pp 126–144
Stavenga DG (1979) Pseudopupils of compound eyes. In: Autrum H (ed) Vision in invertebrates (Handbook of sensory physiology vol. VII/6A). Springer, Berlin Heidelberg New York, pp 357–439
Streck P (1972) Der Einfluss des Schirmpigments auf das Sehfeld einzelner Sehzellen der Fliege *Calliphora erythrocephala* Meig. Z Vergl Physiol 76: 372–402
Vogt K, Kirschfeld K, Stavenga DG (1982) Spectral effects of the pupil in fly photoreceptors. J Comp Physiol 146: 145–152
Washizu Y, Burkhardt D, Streck D (1964) Visual field of single retinula cells and interommatidial inclination in the compound eye of the blowfly *Calliphora erythrocephala*. Z Vergl Physiol 48: 413–428